We are IntechOpen,
the world's leading publisher of
Open Access books
Built by scientists, for scientists

4,800
Open access books available

122,000
International authors and editors

135M
Downloads

Our authors are among the

154
Countries delivered to

TOP 1%
most cited scientists

12.2%
Contributors from top 500 universities

CLARIVATE ANALYTICS
BOOK CITATION INDEX
INDEXED

WEB OF SCIENCE™

Selection of our books indexed in the Book Citation Index
in Web of Science™ Core Collection (BKCI)

Interested in publishing with us?
Contact book.department@intechopen.com

Numbers displayed above are based on latest data collected.
For more information visit www.intechopen.com

Cascaded Nonlinear Optical Mixing in a Noncollinear Optical Parametric Amplifier

Chao-Kuei Lee
Department of Photonics, National Sun Yat-Sen University
Taiwan, R.O.C

1. Introduction

Ultrafast optical science is a rapidly evolving multidisciplinary field: the ability to excite matter with femtosecond light pulses and probe its subsequent evolution on ultrashort time scales opens up completely new fields of research in physics, chemistry, and biology.[1] Furthermore, the high intensities that can be generated using femtosecond light pulses allow us to explore new regimes of light-matter interaction.[2] The implementation of more sophisticated spectroscopic techniques has been accompanied by improvements in laser sources. Considerable effort has been dedicated to the achievement of shorter light pulses,[3-5] to improve temporal resolution; other efforts have worked to expand the frequency tunability of the pulses, since this would make it possible to excite in resonance different materials, and to probe optical transitions occurring at different frequencies. Early sources of femtosecond optical pulses were based on dye laser technology; in that case, some frequency tunability could be achieved by simply changing the laser dye.[6] This flexibility, however, came at the expense of a complicated and time consuming reoptimization.

In recent years, femtosecond laser systems have become readily available. Rapid developments of widely tunable femtosecond laser radiation has also become power tools in the field of ultrafast spectroscopy, especially the transient ultrafast pump-probe spectroscopy on various from small organic compounds to complex enzymes, has opened up new research interests in femto-chemistry and femto-biology in the recent years.[7-9] The combination of high-intensity, ultrashort pulses from amplified solid-state lasers, for example, the regeneratively amplified Ti: sapphire laser systems running at 800-nm, with nonlinear optical techniques, such as optical parametric generator /amplifier (OPG/OPA), has made widely tunable femtosecond laser pulses routinely available in many research laboratories. Generally, the OPG process transfers energy from a high-power, fixed frequency pump beam to a low-power, variable frequency signal beam, thereby generating also a third idler beam. To be efficient, this process requires very high intensities of the order of tens of GW/cm^2; it is therefore eminently suited to femtosecond laser systems, which can easily achieve such intensities even with modest energies, of the order of a few microjoules. They have proved versatile as widely tunable coherent sources, especially for short pulses since they can offer both high gain and high-gain bandwidth. Gain bandwidths of several thousand wave numbers are possible,[10-15] corresponding to transform-limited pulse durations down to a few femtoseconds, and amplification of such short pulses has

been demonstrated.[16,17] In addition, high powers have been generated over a wide range of wavelengths.[18-20]

The techniques are capable of generating widely tunable femtosecond light pulses from the near UV/VIS through the near-IR. [21-49] Among those reports, the seeded non-collinear optical parametric amplifier (NOPA) of whit-light super-continuum is commonly used for generating femtosecond widely tunable radiation.[37-49] The use of a seeder significantly reduces the pumping threshold required spontaneous parametric fluorescence and increases the output energy of OPA, and improves its pulse-to-pulse stability and spatial quality.[42] The use of NOPA has some unique advantages, it allows reduction of group velocity mismatch (GVM), increasing the interaction length between the pump pulse and the seeder and thus increasing the gain factor. However due to the limitation of phase-matching condition, the tuning range of a 400-nm pumped type-I β-BaB$_2$O$_4$ (BBO) NOPA covers only from 460nm to 720nm in the signal branch and from 900nm to 2.4μm in the idler branch. This is unfortunate since tunable femtosecond pulses in the blue-to-near UV region (<460nm) are most useful in many applications ranging from investigation of wide band-gap materials to probing biomolecules. In order to extend the tuning range, various nonlinear optical processes, such as sum frequency generation (SFG) and second harmonic generation (SHG), can be used to convert the output of NOPA to the desired short-wavelength radiation. Petrov *et al.* reported wavelength extension through cascaded 2nd-order nonlinear frequency-conversion process.[24]However, it requires an additional SHG or SFG device for the wavelength conversion. This complicates the entire tunable femtosecond laser system. Furthermore, conversion efficiency of SHG or SFG for NOPA is often limited.

Recently, several groups had demonstrated that femtosecond pulses near 400nm can be generated with a 267-nm-pumped NOPA.[49-52] Using a pump of 258nm from a frequency tripled femtosecond Ti:Sapphire laser system, Tzankvo's group had reported wavelength tunning from 346nm to 453nm. [53] These approaches to generating femtosecond deep UV pulses are typically inefficient and require special and limits conversion efficiency. We recently reported an alternative method of generating tunable femtosecond pulses from 380nm to 465nm near the degenerate point of a 405-nm pumped type-I BBO noncollinearly phase-matched optical parametric amplifier (NOPA).[54,55] This was tentatively attributed to cascading sum frequency generation (SFG) of the generated OPA pulses and the residual fundamental laser pulse at 810nm in the same crystal for NOPA. The tunable SFG output is readily available from the OPA stage without any additional frequency conversion device. In Section 2, we present a theoretically analysis of this much simpler scheme to generate femtosecond tunable radiation. In Section 3, we describe and experimentally demonstrate the arrangement and performance of this approach. Tuning range for various seeding angles, conversion efficiency and pulse profile are characterized in detail. With a pumping energy of 75 μJ at 405 nm, the optical conversion efficiency from the pump to the tunable SFG is more than 5%.

2. Theoretical treatment

Optical parametric amplification belongs to the three-wave frequency mixing processes. In order to achieve efficient frequency conversion, the conservation law of photon energies and momentums must be satisfied in this process [56]:

$$\begin{cases} \hbar\omega_p = \hbar\omega_s + \hbar\omega_i \\ \hbar\vec{k}_p = \hbar\vec{k}_s + \hbar\vec{k}_i \end{cases} \qquad (1)$$

where ω_l and k_l denote the frequency and wave vector of the pump (l=p), signal (l=s) and idler (l=i) beam, respectively. Fig. 1 illustrates the phase matching scheme of the NOPA and cascading SFG to be employed in our setup. The signal beam of NOPA is injected into an appropriate nonlinear optical crystal with an angle α relative to the propagation direction of the pump beam. Here, the sign of α is defined to be positive when the direction of seeding signal beam is rotated counterclockwise from the pump beam. The idler beam is generated at an angle δ with respect to the signal beam. The cascading sum-frequency generation satisfies the following conservation law of energies and momentums:

$$\begin{cases} \hbar\omega_{SFG} = \hbar\omega_i + \hbar\omega_{810} \\ \hbar\vec{k}_{SFG}^{(e)} = \hbar\vec{k}_i^{(o)} + \hbar\vec{k}_{810}^{(o)} \end{cases} \qquad (2)$$

where ω_{810}, k_{810}, ω_{SFG} and k_{SFG} denote the frequency and wave vector of the residual 810-nm pump beam and SFG, respectively. The resulting SFG is an e-ray for a type I BBO-NOPA and propagates with an angle δ' relative to the idler beam direction:

$$\delta' = \tan^{-1}\left(\frac{\vec{k}_{810}^{(o)}\sin\delta}{\vec{k}_{810}^{(o)}\cos\delta + \vec{k}_i^{(o)}} \right)$$
$$\delta = \theta_i - \theta_s \qquad (3)$$

where θ_s, θ_i are the angle of signal and idler with respect to the optic axis, respectively. The angle θ between the SFG beam and optic axis can be calculated from

$$\theta = \theta_i - \delta' \qquad (4)$$

The index of refraction experienced by the SFG shall be

$$n_{SFG}^{(e)} = \frac{n_{SFG}^{(o)}n_{SFG}^{(e)}}{\sqrt{\left(n_{SFG}^{(o)}\sin\theta\right)^2\left(n_{SFG}^{(e)}\cos\theta\right)^2}} \qquad (5)$$

To properly depict the phase mismatching of the three-wave mixing processes in the NOPA and SFG, we express the summation of the wave vectors of optical pulses as:

$$\begin{cases} \Delta\vec{k} = \vec{k}_p - \vec{k}_s - \vec{k}_i \\ \Delta\vec{k} = \vec{k}_{SFG} - \vec{k}_{810} - \vec{k}_i \end{cases} \qquad (6)$$

Upon the equations presented above, we can calculate the central wavelength and the tuning range of cascading SFG at various seeding angles by taking into account the phase-matching condition for both NOPA and SFG and the group velocity mismatch (GVM) among the optical pulses involved. Fig. 2 presents the tuning range of cascading SFG at various seeding angles α. When the seeding angle ranges from -3° to -18°, the phase-matching angle of the NOPA was found to overlap with that for SFG in a ~400nm-pumped

type-I BBO-NOPA near its degenerate point of θ~29°. The result reveals that the central wavelength of the cascading SFG is adjustable from 410nm to 440nm by decreasing the seeding angle (see the filled squares for Δk=0). The tuning of the DFG can be achieved in two ways: one is to change the seeding angle between the white light supercontinuum (WLS) and the pump, the other is to scan the orientation of the crystal.
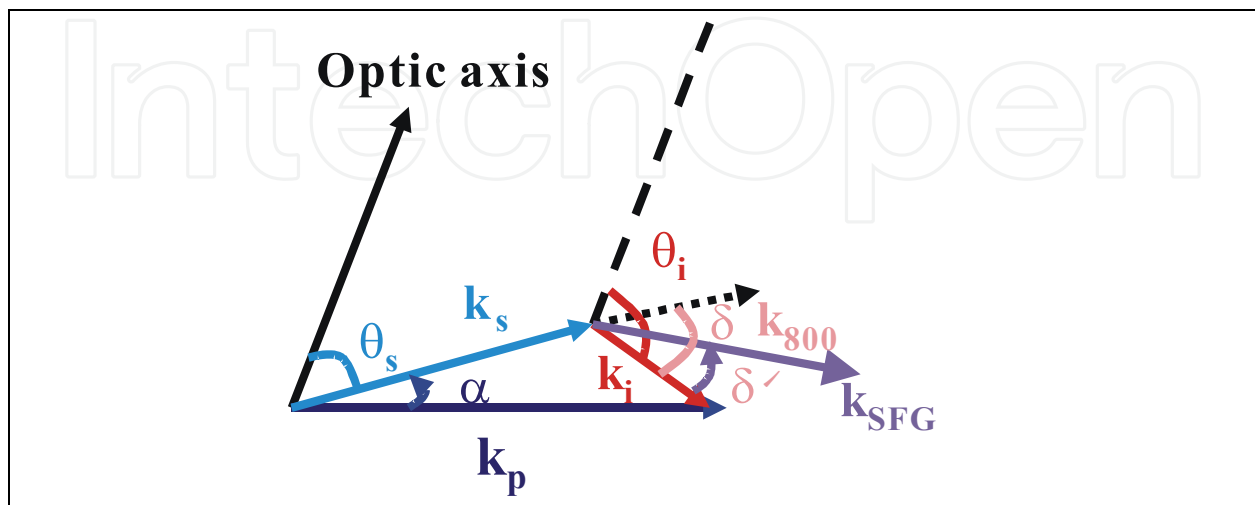

Fig. 1. Schematic showing the noncollinear phase matching condition for optical parametric amplifier (OPA) and the cascading SFG of OPA and residual 810nm pump beam.

As can be seen in Fig. 2 that at larger seeding angles, such as -15°, where the central wavelength with Δk=0 is near 410nm, small GVM and therefore large pulse interactive length are yielded for wavelength from 380nm to ~460nm. At seeding angle around -8°, the tuning range slightly increases and covers from ~390nm to ~500nm. At an even small angle such as -2° →-6°, the tuning range breaks into two separated regimes. But at such a small seeding angle, the GVM is large and the pulse interaction length becomes shorter. We need to apply higher pumping intensity in order to generate stable SFG. In addition to the
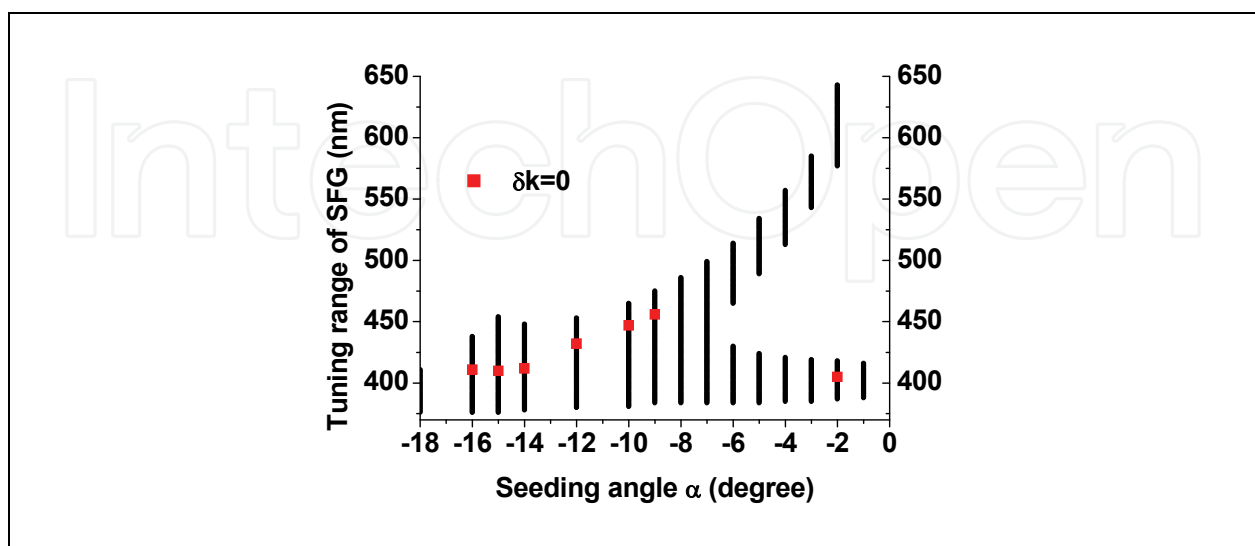

Fig. 2. Theoretical tuning curves of the cascading SFG at various seeding angles between OPA and residual 810-nm laser beam in a 405nm pumped type-I BBO-NOPA

drawback, the GVM from dispersion of WLS is also difficult to be compensated with the noncollinear phase matching scheme. At a given seeding angle, the SFG wavelength can also be tuned by changing the orientation of the NOPA crystal and thus continuous wavelength scan can be done.

3. Experimental setup

The experimental setup is shown in Fig. 3. An amplified femtosecond Ti: sapphire laser provides pulse energy of 1mJ at 810nm with pulse duration of ~90 fs and 1-kHz pulse repetition frequency. The output of the laser is split into two parts: 90% of the energy is frequency-doubled to 405nm with a 0.30-mm-thick BBO for pumping NOPA. The frequency-doubling pulse energy is adjustable from 50 to 120 μJ. The rest 10% of the Ti:sapphire laser beam is used to generate WLS with a 2-mm-thick CaF_2 plate. CaF_2 plate is employed to reduce the chirping in WLS and increase the seeding intensity so that the generated OPA pulses could be stronger and more stable. The generated WLS is collimated and then temporally and spatially overlaps with the SH beam in a 2-mm-long type-I BBO cut at 29o. The beam crossing angle between the seeding and the pump pulses is adjustable from -2o to -18o.

Around the degenerate point of the NOPA, a bright beam with wavelength tunable from near UV to the blue can readily be observed. The inset of Fig. 3 was taken with the output of the NOPA being projected onto a while paper. The ring is the parametric superfluorescence and the black spot at the center of the ring indicates the position of the residual pump beam at 405nm. We punched a hole on the screen to let the residual pump beam pass through the hole to avoid saturation of CCD camera by the scattered residual pump beam. The red spot on the right-hand side of the pump and near the superfluorescence ring is the output of OPA. On the left-hand side of the pump, the spot outside of the ring is originated from the tunable SHG of the OPA component and the bright spot inside of the ring is widely tunable from 380 nm to 460 nm.
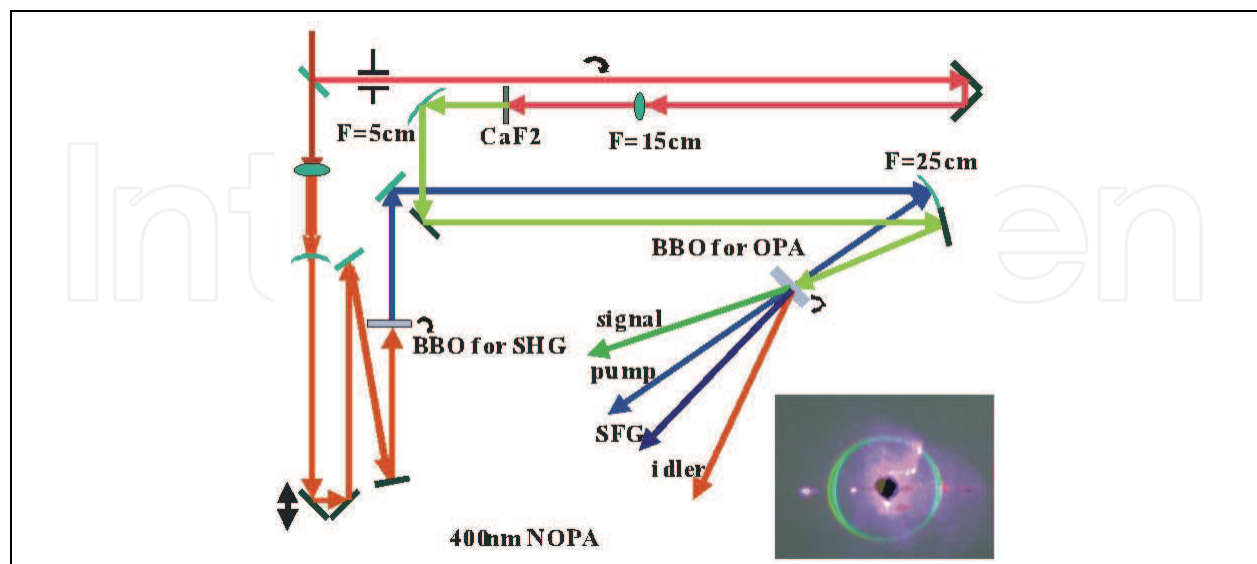

Fig. 3. Experimental setup of the noncollinear optical parametric amplifier and cascading SFG employed in this study. The inset shows the beam pattern of NOPA output projected onto a white screen. The image was taken with a seeding angle of -8o.

4. Results and discussions

We found experimentally that the bright and widely tunable spot at UV/blue can be attributed to the sum-frequency-generation (SFG) from the NOPA and the residual pump beam at 810 nm used in WLS generation. At seeding angle of -14°, the SFG was observable even below the pumping threshold of parametric superfluorescence. However when the seeding angle is decreased to -6°→-8°, we have to pump the NOPA crystal to a level at which a bright and stable parametric super fluorescence is obtained. To further reduce the seeding angle, the SFG becomes difficult to be generated. Based on the calculation of the GVM among SFG, OPA and 810-nm pulses, we found that seeding angle between -8.4° and -14° is most appropriate for the cascading SFG. At a small seeding angle of ~-1.5°, the large GVM leads to a short interactive length in the crystal and it weakens the cascading SFG. Note that at the small seeding angle we can still observe several blue spots, which could be attributed to the SHG of the OPA and cascading SFG. As shown in Fig. 4, at a small seeding angle of ~-2°, the phase matching curve of the cascading SFG crosses with that of the SHG of the idler with a wavelength near 800 nm. Therefore, it is possible to simultaneously observe the SHG of the NOPA idler wave and cascading SFG at small seeding angle. Although the SHG of NOPA allows extending the wavelength to 380-nm or lower, its output energy is significantly lower than the cascading SFG at large seeding angle.
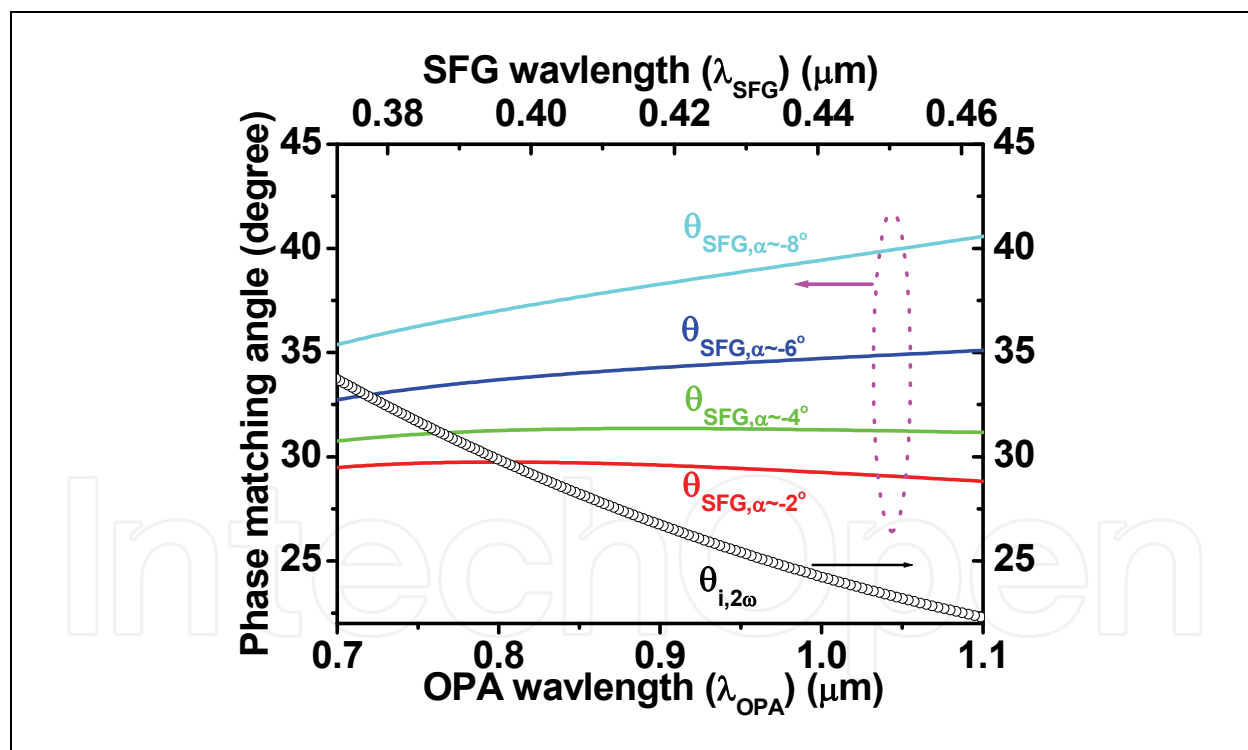

Fig. 4. Calculated curves of phase-matching angle of the cascading SFG (left y-axis) and the SHG of NOPA idler wave (right y-axis) as a function of optical wavelength of OPA (x-axis: bottom) and SFG (x-axis: top).

4.1 Tuning range of cascaded SFG and SHG

We can adjust the central wavelength of the cascading SFG by varying the orientation of the NOPA crystal with a given seeding angle. Fig. 5 shows the spectra of the cascading SFG

with a seeding angle of -8.4^o and -14°, respectively. As shown in Fig. 5(a) with a seeding angle of -8.4^o, the tuning range covers from 395nm to 465nm and similarly with seeding angle of -14° the tuning range can extend from 380nm to 432nm. Figure 6 shows the tuning characteristics of the generated SFG and SHG, respectively, at a seeding angle of 8-degree. The SFG is tuned by rotating the BBO crystal. A tuning range from 389 nm to 425-nm had been observed as shown in the top figure. The maximum output of SFG is at 400-nm. With the same seeding angle of 8 degree, the tuning range of the cascaded SHG of OPA covers a very broad spectral range from 410-nm to 660-nm. The maximum output occurs at 439-nm. The bottom figure shows the spectra of the tunable SHG at various angles of the BBO.

(a)

(b)
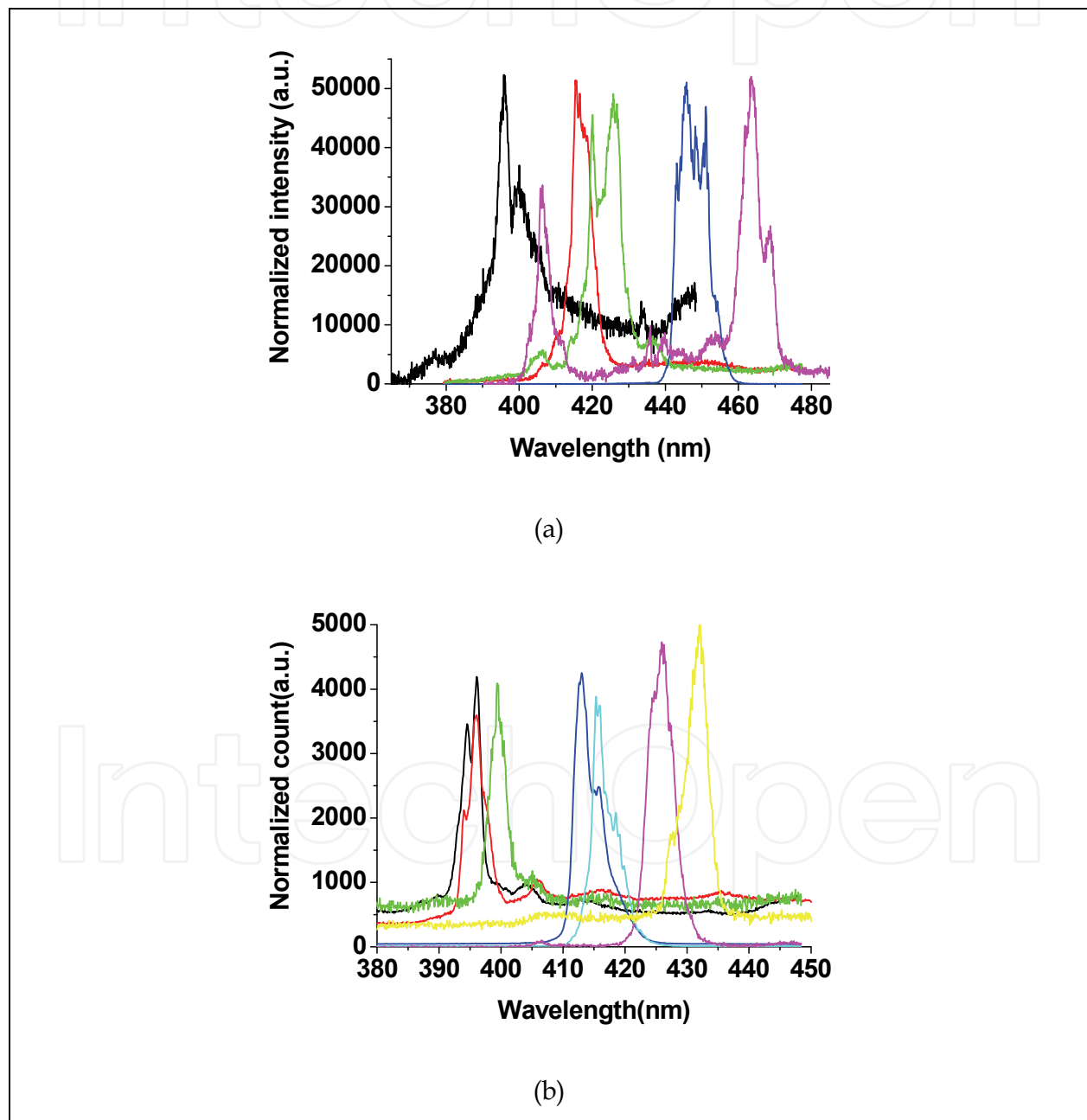
Fig. 5. Spectrum of the cascading SFG at various orientations of BBO. The seeding angle used is (a)~-8.4^o; (b)~-14°

Figure 6 shows the tuning characteristics of the generated SFG and SHG, respectively, at a seeding angle of 8-degree. The SFG is tuned by rotating the BBO crystal. A tuning range from 389 nm to 425-nm had been observed as shown in the top figure. The maximum output of SFG is at 400-nm. With the same seeding angle of 8 degree, the tuning range of the cascaded SHG of OPA covers a very broad spectral range from 410-nm to 660-nm. The maximum output occurs at 439-nm. The bottom figure shows the spectra of the tunable SHG at various angles of the BBO. It is seen from Fig. 2 that the tuning range of the cascaded SFG/SHG fills the gap of the tuning range of a 400-nm pumped OPA in the wavelength range shorter than 460-nm. Experimentally, it is observed that the SFG and SHG can be generated simultaneously over a broad tuning range of the OPA.
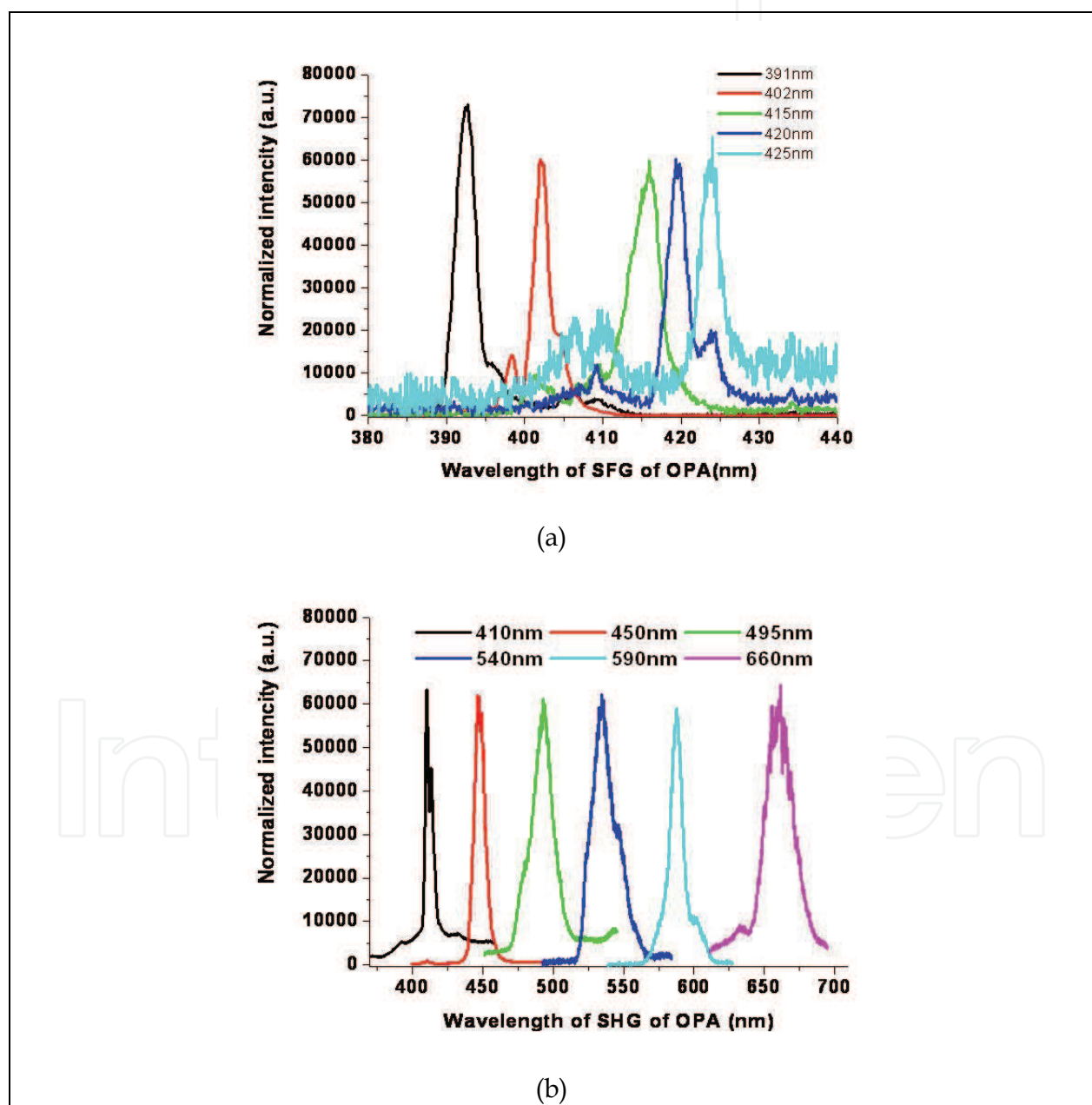

(a)

(b)

Fig. 6. Spectra of cascaded SFG (up-figure) and SHG (bottom-figure) of NOPA at various BBO orientations. The spectra were taken at a seeding angle of 8 degree.

In order to understand such a phenomenon, a theoretical calculation was done to find the phase-matching conditions for the OPA, the cascaded SFG and SHG. It can be shown that when the seeding angle lies between 3 to 18 degrees, the phase-matching angle of the cascaded SFG and SHG of OPA is coincidently overlapped with that of a 400-nm pumped type-I BBO NOPA at its degenerate point. Fig. 7 shows the theoretical tuning range and the SFG wavelength with $\Delta k=0$ for a variety of seeding angle α. The measured wavelengths with $\alpha = -8.4^o$ and -14° are also included for comparison. It was found that the experimental results (open symbols) agree well with the theoretical calculation (solid lines). The measured SFG wavelength with maximum-gain (the star symbols) also coincides well with the calculated phase-matched SFG wavelength with $\Delta k=0$ (the filled squares). This firmly supports our concept about the origin of the generated tunable UV/blue radiation from NOPA.
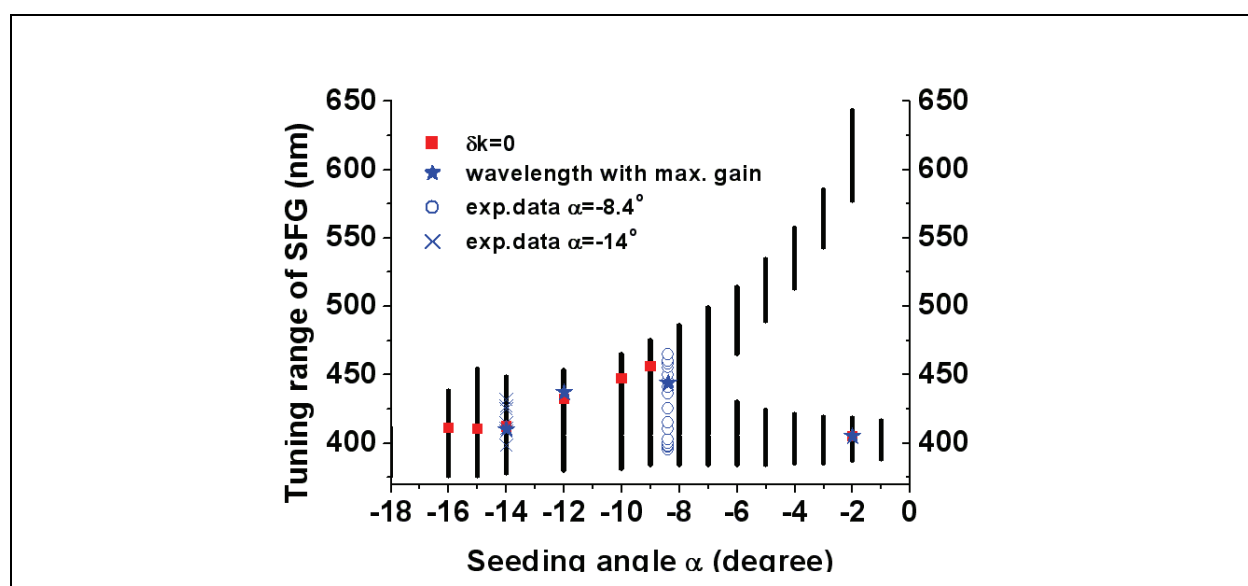

Fig. 7. Theoretical tuning range and the cascading SFG wavelength with maximum gain under various angles of α. Experimental data of SFG wavelength with seeding angle of -8.4^o and -14° are also included for comparison.

4.2 Conversion Efficiency of Cascaded SFG-OPA

The cascading SFG yields fairly high optical conversion efficiency. With a pumping energy of 75 μJ per pulse, the output of the SFG was measured to be about 4μJ, which corresponds to an optical conversion efficiency of more than 5% from the pump to the SFG. The output of DFG can be increased by increasing the total energy used for WSL generation and thus the residual radiation at 810-nm is higher. Fig. 8 presents a plot of the SFG output power at a variety of residual pulse energy at 810nm along the WLS seeding beam. The observed linear dependence of SFG output power on residual 810nm beam provides extra supporting data for our notion of the generation mechanism of the cascading SFG. As noted above, we can also produce tunable near UV-VIS femtosecond pulses by frequency-doubling the output of the OPA or use SFG to combine the output of OPA with the fundamental laser at ~810nm. However, these schemes need extra NLO

crystal and require synchronous tuning of at least two crystals. This makes the operation of these devices complicated.
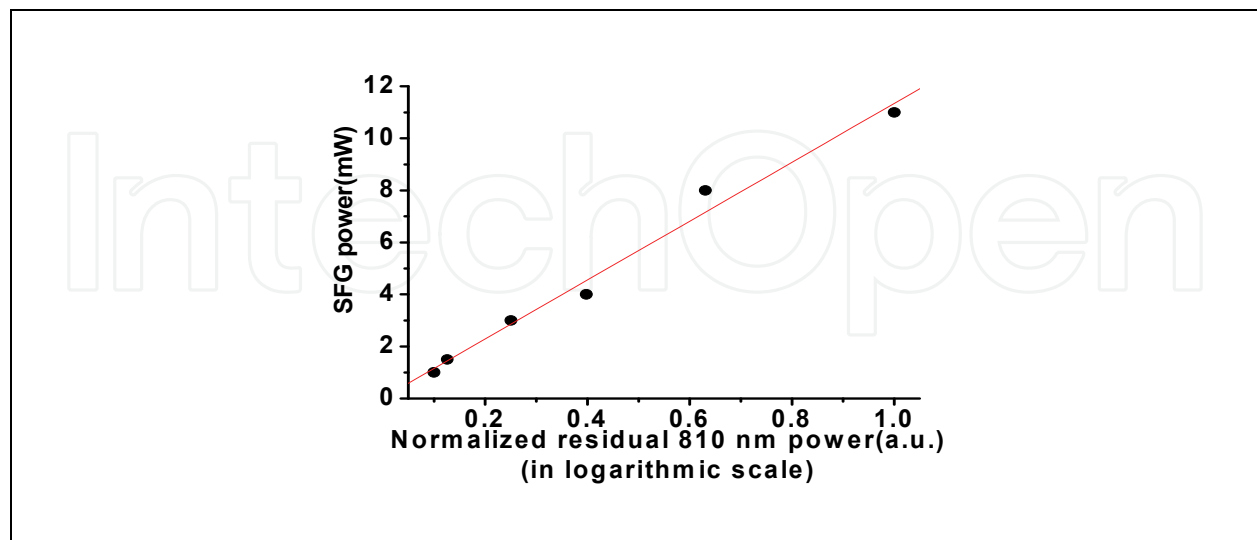

Fig. 8. Output power of the cascading SFG as a function of the averaged power of the residual 810nm pump beam

4.3 Pulse shape of SFG

By using a newly developed OPA-based frequency-resolved optical gating (OPA-FROG) [57], the output of the NOPA can be fully characterized. Fig. 9 shows the measured OPA-FROG trace and its retrieved amplitude and phase of the NOPA component at 571nm. The retrieved OPA-FROG trace shows that no significant chirping in the NOPA output pulse. The pulse duration of the NOPA is about 75-fs. We also employ a single-shot XFROG[58] to deduce the pulse profile of the cascading SFG and found the FWHM duration is about 100-fs. The value is longer than that of the corresponding NOPA but shorter than that of the residual 810-nm pulse. This result also agrees with the notion that the SFG component is a temporal convolution of the NOPA component and the residual fundamental beam. The OPA component is generally shorter than that of its pump at 405-nm, which is shorter than its fundamental pulse at 810 nm.

5. Summary

In conclusion, we have successfully demonstrated the generation of femtosecond laser pulses tunable from 380nm to 460nm via cascading SFG in a 405nm pumped type-I non-collinearly phase-matched OPA. Furthermore, we theoretically analyzed this much simpler scheme to generate femtosecond tunable radiation. Tuning range at various seeding angles, conversion efficiency and pulse profile are characterized in detail. The energy conversion efficiency of the SFG is more than 5%. The reported scheme provides a simple while effective way to extend the tuning range of a 405nm pumped type-I BBO-OPA from 460nm down to 380nm without any additional frequency up-conversion stage. It is also found that the beam quality and pulse shape of the SFG component is about the same as that of OPA.
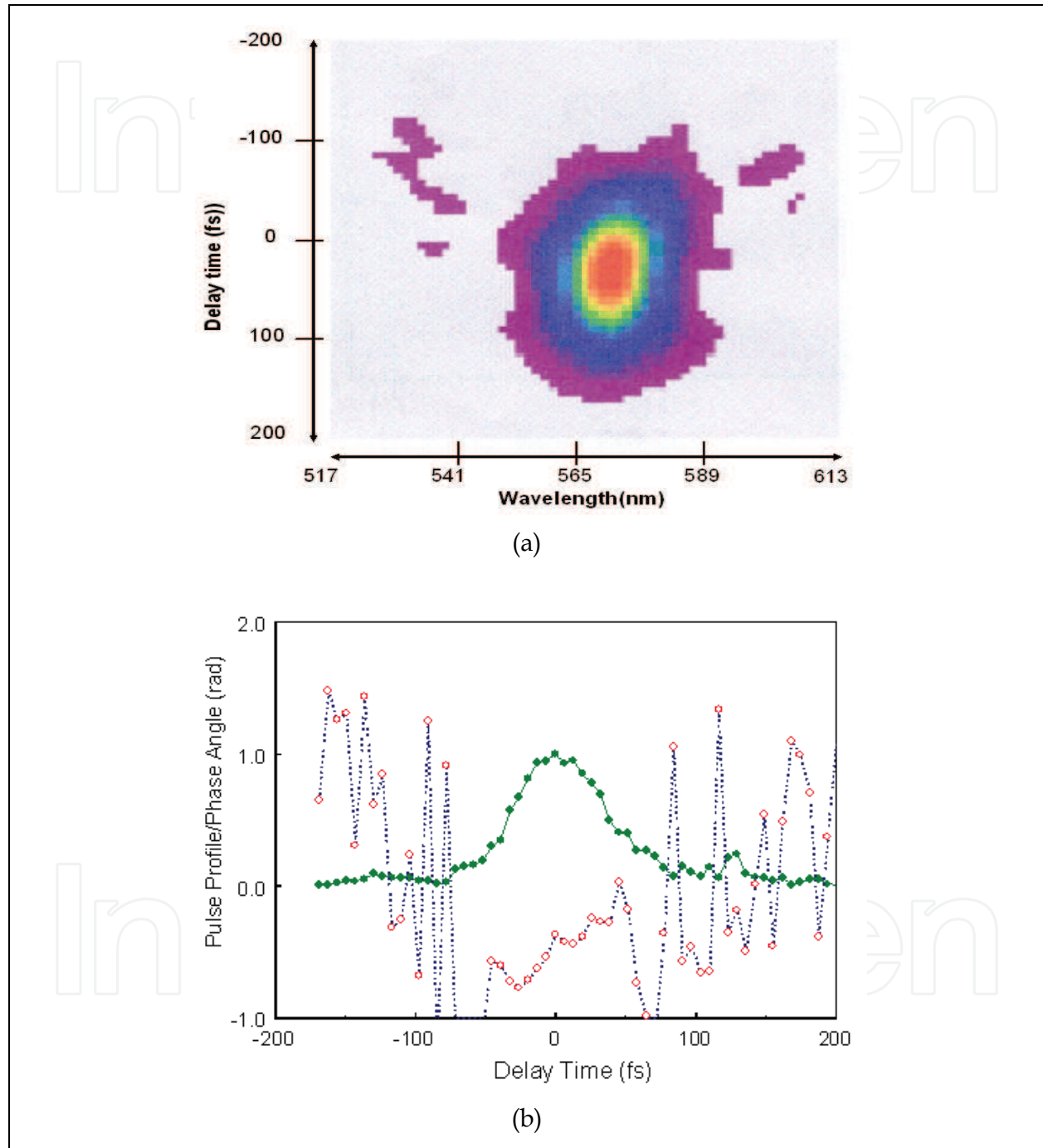
(a)

(b)

Fig. 9. (a) Measured OPA-FROG trace of NOPA output at 571 nm; (b) the retrieved pulse profile (solid line) and phase (dotted line) of the NOPA output.

6. References

[1] For a overview of the state of the art of ultrafast spectroscopy, see for example: Ultrafast Phenomena XII, Springer Verlag Series in Chemical Physics Vol. 66, edited by T. Elsaesser, S. Mukamel, M. M. Murnane, and N. F. Scherer ~Springer, Berlin, 2001.

[2] T. Brabec and F. Krausz, Rev. Mod. Phys. 72, 545 ~2000

[3] J. P. Zhou, G. Taft, C. P. Huang, M. M. Murnane, H. C. Kapteyn, and I. P. Christov, Opt. Lett. 19, 1149 ~1994

[4] A. Stingl, M. Lenzner, C. Spielmann, F. Krausz, and R. Szipocs, Opt. Lett. 20, 602 ~1995.

[5] G. Steinmeyer, D. H. Sutter, L. Gallmann, N. Matuschek, and U. Keller, Science 286, 1507 ~1999.

[6] R. L. Fork, B. I. Greene, and C. V. Shank, Appl. Phys. Lett. 38, 671 ~1981.

[7] A. H. Zewail, J. Phys. Chem. A 104, 5660 (2000)

[8] N. H. Damrauer, G. Cerullo, A. Yeh, T. R. Boussie, C. V. Shank, J. K. McCusker, Science 275, 54 (1997).

[9] T. Elsaesser, S. Mukamel, M. Murnane, N. F. Scherer, Ultrafast Phenomena XII, in: Proceedings of the 12th International Conference, Springer, New York, 2000.

[10] P. Di Trapani, A. Andreoni, C. Solcia, P. Foggi, R. Danielius, A. Dubietis, and A. Piskarskas, J. Opt. Soc. Am. B 12, 2237–2244 (1995).

[11] J. M. Liu, G. Zhou, and S. J. Pyo, J. Opt. Soc. Am. B 12, 2274–2287 (1995).

[12] R. Danielius, A. Piskarskas, A. Stabinis, G. P. Banfi, P. Di Trapani, and R. Righini, J. Opt. Soc. Am. B 10, 2222–2232 (1993).

[13] A. Piskarskas, A. Stabinis, and A. Yankauskas, 'Sov. Phys. Usp. 29, 969–979 (1986).

[14] R. Danelius, A. Piskarskas, V. Sirutkaitis, A. Stabinis, and A. Yankauskas, JETP Lett. 42, 122–124 (1985).

[15] J. Wang, M. H. Dunn, and C. F. Rae, Opt. Lett. 22, 763–765 (1997).

[16] A. Shirakawa, I. Sakane, H. Takasaka, and T. Kobayashi, 'Appl. Phs. Lett. 74, 2268–2270 (1999).

[17] G. Cerullo, M. Nisoli, S. Stagira, and S. De Silvestri, Opt. Lett. 23, 1283–1285 (1998).

[18] I. N. Ross, J. L. Collier, P. Matousek, C. N. Danson, D. Neely, R. M. Allott, D. A. Pepler, C. Hernandez-Gomez, and K. Osvay, Appl. Opt. 39, 2422–2427 (2000).

[19] F. Rotermund, V. Petrov, and F. Noack, Opt. Commun. 169, 183–188 (1999).

[20] K. Osvay, G. Kurdi, J. Klebniczki, M. Csatari, I. N. Ross, E. J. Divall, C. J. Hooker, and A. J. Langley, Appl. Phys. B 74, 163–169 (2002).

[21] J. Opt. Soc. Am. B 8 , 2087 (1991).

[22] R. Danielius , A. Piskarskas , A. Stabinis , G. P. Banfi , P. Di Trapani , and R. Righini , J. Opt. Soc. Am. B10 , 2222 (1993)

[23] F. Seifert, V. Petrov , and F. Noack , Opt. Lett. 19, 837 (1994).

[24] V. Petrov., F. Seifer, O. Kittlemann, J. Ringling, F. Noack, , J. Appl. Phys. 76, 7704 (1994)

[25] V. V. Yakovlev , B. Kohler , and K. R. Wilson , Opt. Lett. 19, 2000 (1994).

[26] M. Nisoli , S. De Silvestri , V. Magni , O. Svelto , R. Danielius , A. Piskarskas , G. Valulis, and A. Varanavicius , Opt. Lett. 19, 1973 (1994).

[27] V. Petrov, F. Seifert, and F. Noak, Appl. Phys. Lett. 65, 268 (1994).

[28] V. Petrov , F. Seifert , and F. Noak, Appl. Opt. 33 , 6988 (1994).

[29] M. K. Reed, M. K. Steiner-Shepard, and D. K. Negus, Opt. Lett.19, 1855-1857 (1994).

[30] S. R. Greenfield and M. R. Wasielewski, Appl. Opt. 34, 2688-2691 (1995).

[31] Opt. Lett. 20, 1394 (1995).

[32] R. Danielius , A. Piskarskas , P. Di Trapani , A. Andreoni , C. Solcia , and P. Foggi , Appl. Opt. 35 , 5336 (1996)

[33] P. Matousek , A. W. Parker , P. F. Taday , W. T. Toner , and M. Towrie, Opt. Commun. 127, 307-312 (1996).

[34] K. S. Wong, H. Wang, G. K. Wong and J. Y. Zhang, Appl. Opt. 36, 1889, (1997).

[35] P. Di. Trapani, A. Andreroni, C. Solicia, G. P. Banfi, R. Danielius, A. Piskarskas, P. Foggi, J. Opt. Soc. Am. B 14, 1245 (1997).

[36] J. Y. Zhang, Z. Y. Xu, Y. F. Kong , Chaowen Yu, and Yichen Wu, Appl. Opt. 37, 3299-3305 (1998).

[37] P. Di Trapani , A. Andreoni , P. Foggi , C. Solcia , R. Danielius , and A. Piskarskas , Opt. Commun. 119, 327-332 (1995).

[38] P. Di Trapani , A. Andreoni , G. P. Banfi , C. Solcia , R. Danielius , P. Foggi , M. Monguzzi , A. Piskarskas , and C. Sozzi , Phys. Rev. A 51, 3164 (1995).

[39] T. Wilhelm, J. Piel, and E. Riedle, Opt. Lett. 22, 1494-1496 (1997).

[40] G. Cerullo, M. Nisoli, and S. De Silvestri, Appl. Phys. Lett. 71, 3616-3618 (1997).

[41] G. Cerullo, M. Nisoli, S. Stagira, and S. De Silvestri, Opt. Lett. 23, 1283-1285 (1998).

[42] V. Krylov, O. Ollikainen, J. Gallus, U. Wild, A. Rebane, A. Kalintsev, Opt. Lett. 23, 100-102 (1998)

[43] A. Shirakawa and T. Kobayashi, Opt. Lett. 23, 1292-1294 (1998).

[44] F. Rotermund, V. Petrov and F. Noack, Optics Communs., 171, 183-188, (1999).

[45] E.. Riedle, M. Beutter, S. Lochbrunner, J. Piel, S. Schenkl, S. Sporlein, W. Zinth, Appl. Phys. B 71, 457 (2000).

[46] J. Piel, M. Beutter, E. Riedle, Opt. Lett., 25, 180-182 (2000).

[47] Howe-Siang Tan, Warren S. Warren, Elmar Schreiber, Opt. Lett. 26, 1812-1814 (2001)

[48] R. Huber, H. Satzger, W. Zinth, and J. Wachtveitl, Opt. Commun., 194, 443-448 (2001).

[49] P. Tzankov, I. Buchvarov, T. Fiebig, Opt. Commun., 203, 107-113 (2002).

[50] K. Osvay, G. Kurdi, J. Klebniczki, M. Csatari, and I. N. Ross, Appl. Phys. Lett. 80, 1704 ~2002!.

[51] K. Osvay, G. Kurdi, J. Klebniczki, M. Csatari, I. N. Ross, E. J. Divall, C. H. J. Hooker, and A. J. Langley, Appl. Phys. B: Lasers Opt. B74, S163~2002.

[52] K. Osvay, G. Kurdi, J. Klebniczki, M. Csatari, I. N. Ross, E. J. Divall, C.H. J. Hooker, and A. J. Langley, in Proceedings of the Conference on Lasers and Electro-optics, 18–22 June, Munich, Germany ~2001!.

[53] P. Tzankov, T. Fiebig, and I. Buchvarov, in Proceedings of the International Quantum Electronics Conference, 22–28 June, Moscow, Russia ~2002.

[54] Chao-Kuei Lee, Jing-Yuan Zhang[+], J. Y. Huang and Ci-Ling Pan, Optics Express 11, 1702-1708 (2003).

[55] Chao-Kuei Lee, Jing-Yuan Zhang, J. Y. Huang and Ci-Ling Pan, *JOSA-B*. 21, 1494-1499 (2004).

[56] Y.R. Shen, "Principal of Nonlinear Optics", (John Wiely & Sons, 1984).

[57] J. Y. Zhang, Aparna Prasad Shreenath, Mark Kimmel, Erik Zeek and Rick Trebino, and
        Stephan Link, Optics Express, 11, 601-609 (2003).

[58] Jing-Yuan Zhang, Chao-Kuei Lee, Jung Y. Huang and Ci-Ling. Pan, *Optics Express* 12,
        574-581 (2004)
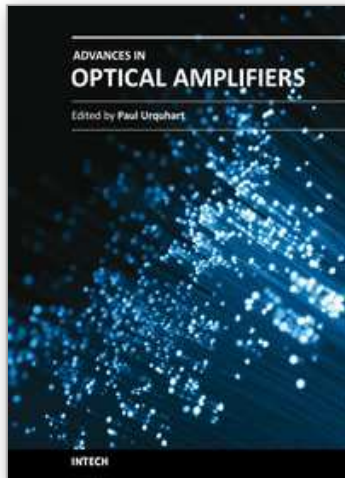
Advances in Optical Amplifiers
Edited by Prof. Paul Urquhart

Optical amplifiers play a central role in all categories of fibre communications systems and networks. By compensating for the losses exerted by the transmission medium and the components through which the signals pass, they reduce the need for expensive and slow optical-electrical-optical conversion. The photonic gain media, which are normally based on glass- or semiconductor-based waveguides, can amplify many high speed wavelength division multiplexed channels simultaneously. Recent research has also concentrated on wavelength conversion, switching, demultiplexing in the time domain and other enhanced functions. Advances in Optical Amplifiers presents up to date results on amplifier performance, along with explanations of their relevance, from leading researchers in the field. Its chapters cover amplifiers based on rare earth doped fibres and waveguides, stimulated Raman scattering, nonlinear parametric processes and semiconductor media. Wavelength conversion and other enhanced signal processing functions are also considered in depth. This book is targeted at research, development and design engineers from teams in manufacturing industry, academia and telecommunications service operators.

INTECH

open science | open minds